On the Generation of Convectively Driven Mesohighs Aloft

J. M. FRITSCH[1] AND J. M. BROWN

Office of Weather Research and Modification, NOAA, Environmental Research Laboratories, Boulder, CO 80303

(Manuscript received 4 February 1982, in final form 29 July 1982)

ABSTRACT

In an attempt to determine the relative contribution of the direct incorporation of cold air (detrainment from overshooting convective cloud tops) to the production of mesohighs in the vicinity of the tropopause, two numerical simulations were performed using a 20 km horizontal resolution, 20-level primitive equation model. One simulation included direct cooling and the other did not. The results showed that including the cooling increased the high-level pressure and wind perturbations by approximately 30 and 40%, respectively. The simulation results also showed that in spite of the omission of the direct cloud cooling, a high-level cold pool was still generated. The cooling was accomplished by adiabatic expansion in response to the lifting by the convectively driven *mesoscale* vertical circulation. Thus, it appears that the mesoscale adiabatic expansion is the dominant effect in elevated-mesohigh production and the detrainment of overshooting air is an important modifying factor.

1. Introduction

It has been recognized for many years that intense convectively-driven weather systems in the tropics, including cloud clusters, tropical storms and hurricanes, are commonly associated with meso-α scale outflow anticyclones in the upper troposphere (Riehl, 1959; Yanai, 1964; Fett, 1966; Kotswaram, 1967; Black and Anthes, 1971; Leary, 1979; Houze and Betts, 1981; Gamache and Houze, 1982). That similar structures occur frequently in mid-latitudes over the central and eastern United States during late spring and summer has been systematically documented by Ninomiya (1971a,b), Fritsch and Maddox (1981a) and Maddox (1980b). These features are commonly associated with so-called mesoscale convective complexes (MCC's; see Maddox, 1980a), an example of which is shown in Fig. 1. The wind barbs on this figure, representing errors in the 12 h wind forecast from the Limited-area Fine-mesh Model[2] show the characteristic anticyclone outflow resulting from the intense, concentrated convective activity. Fritsch and Maddox (1981a) show that the strength and character of this error pattern in Fig. 1 is typical at 200 mb in the vicinity of MCC's, largely because the LFM is incapable of correctly predicting MCC occurrence. Other means of isolating the upper flow associated with MCC's, for example the scale-separation analysis technique discussed by Maddox (1980b), also revealed the prominence of anticyclonic outflow near 200 mb (see Fritsch and Maddox, 1981a).

What causes this anticyclonic outflow? The most plausible explanation is that it results from a condition of geostrophic imbalance on the mesoscale in upper-tropospheric, lower-stratospheric flow, due to the presence of a relative maximum of pressure (on a constant height surface in the upper troposphere) in the area of active convection. In a mature, quasi-steady hurricane, the imbalance is probably principally a consequence of the rapid (relative to a geostrophic-adjustment time) change in horizontal pressure-gradient force felt by air parcels transported vertically by the hurricane's mesoscale circulation. In the case of MCC's, the time scale of their development and decay is such that even air parcels in their vicinity which do not move vertically may experience large, rapid changes in pressure-gradient force as a pressure perturbation develops in the upper troposphere.

Linear analyses of a resting base state having a conditionally unstable lapse rate show that, for realistic profiles of parameterized heating by convection, amplifying perturbations possess a warm core with high pressure (or high height on a constant pressure surface) aloft above deepening low pressure at low levels (Syōno and Yamasaki, 1966; Koss, 1976). Numerical models of hurricanes (Ooyama, 1969; Rosenthal, 1969; Jones, 1980; and others) show a similar tendency—development of an outflow anticyclone aloft which becomes annular shaped (surrounding the up-

[1] Present affiliation: Department of Meteorology, The Pennsylvania State University, University Park, PA 16802.

[2] This model, known as the LFM, is run operationally twice daily at the National Meteorological Center. It has a horizontal resolution of 135 km.

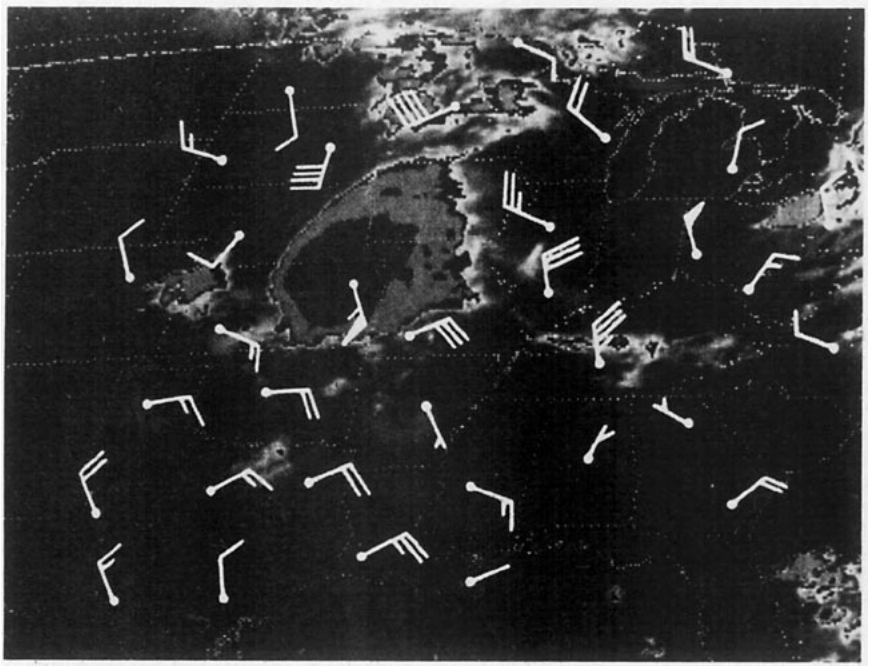

FIG. 1. Infrared satellite imagery of mesoscale convective complex at 1200 GMT 28 June 1979. Wind barbs are vector errors of the 12 h LFM predicted 200 mb wind field. Full wind barb = 5 m s^{-1}; flag = 25 m s^{-1}.

per reaches of the core region where cyclonic outflow prevails) as the hurricane develops. Mesoscale numerical simulations in middle latitudes incorporating the effects of convection (Kreitzberg and Perkey, 1977; Fritsch and Maddox 1981b; Maddox *et al.*, 1981) have also produced upper-tropospheric mesohighs. In none of the numerical simulations, however, have the dynamics of the development of the upper-tropospheric, lower-stratospheric mesohigh been systematically explored. The present paper represents a small contribution toward this end.

2. Possible causes of mesohigh development

We consider several possible mechanisms which could contribute to formation of upper-tropospheric mesohighs.

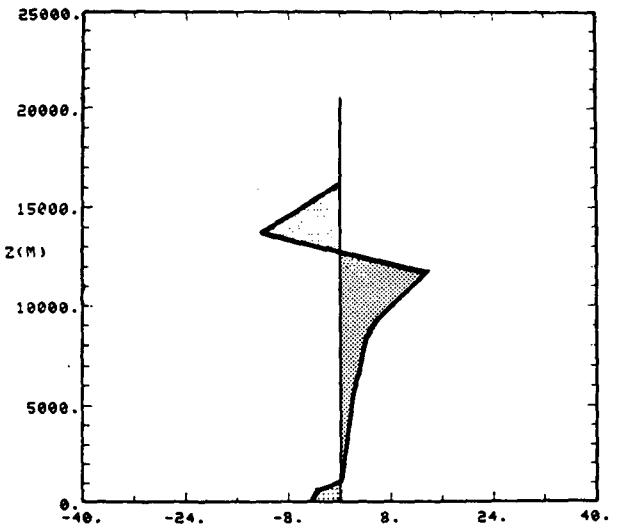

FIG. 2. Typical vertical distribution of convective cloud heating (°C h^{-1}) at a numerical model grid point.

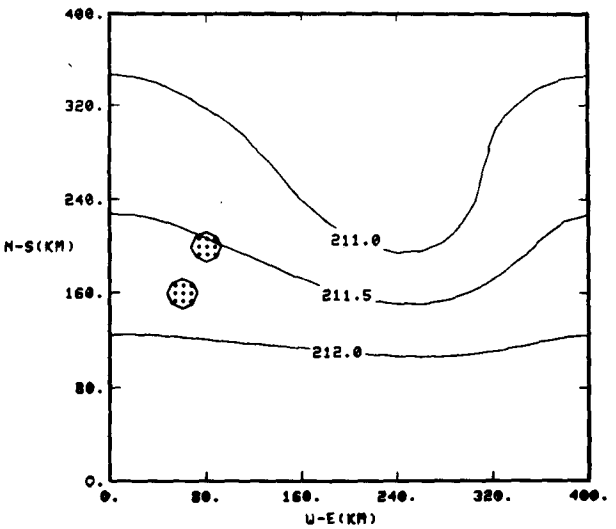

FIG. 3. Pressure (mb) at 11.8 km level and area of active convection (stippled) 15 min after convection begins.

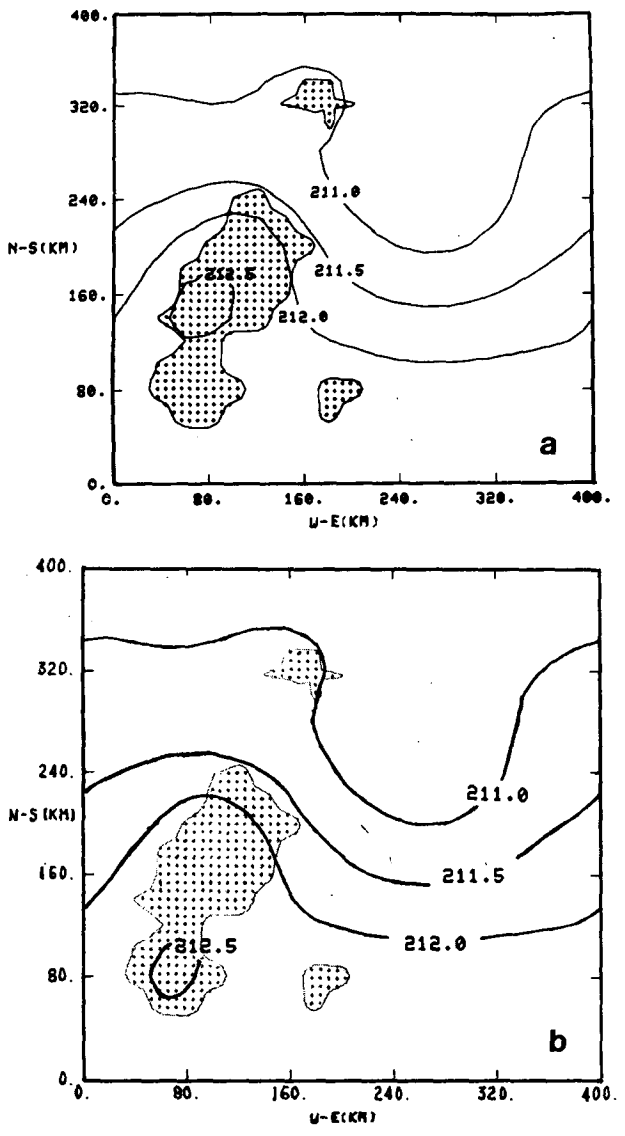

FIG. 4. As in Fig. 3 except 45 min after convection began. In (a) cooling by overshooting cloud tops is included; in (b) it is omitted.

a. Injection of cold turbulent air near or above the tropopause by penetrative cumulonimbus updrafts

In this process, cumulonimbus updrafts penetrating above (overshooting) their equilibrium level (typically near the tropopause) "detrain" cold, turbulent air into the upper troposphere or lower stratosphere, resulting in a mesoscale cold anomaly. In a sense this process is crudely analogous to the growth of the daytime convective mixed layer due to surface heating (Deardorff, 1974); i.e., overshooting by dry convective thermals leads to a slight negative temperature anomaly (relative to the predawn temperature profile) at the top of the surface-based mixed layer. Because the cooling near the tropopause is restricted to a mesoscale area of convection, it will force a hydrostatically consistent *mesoscale* pressure perturbation with maximum pressure below the layer of maximum cooling. This explanation is suggested by the anomalously low temperatures found at lower stratospheric levels above MCC's (see Fritsch and Maddox, 1981a) and above tropical cloud clusters in the vicinity of Indonesia (R. H. Johnson, 1981, personal communication). Apparently Kotswaram (1967) was the first to propose this mechanism to account for observa-

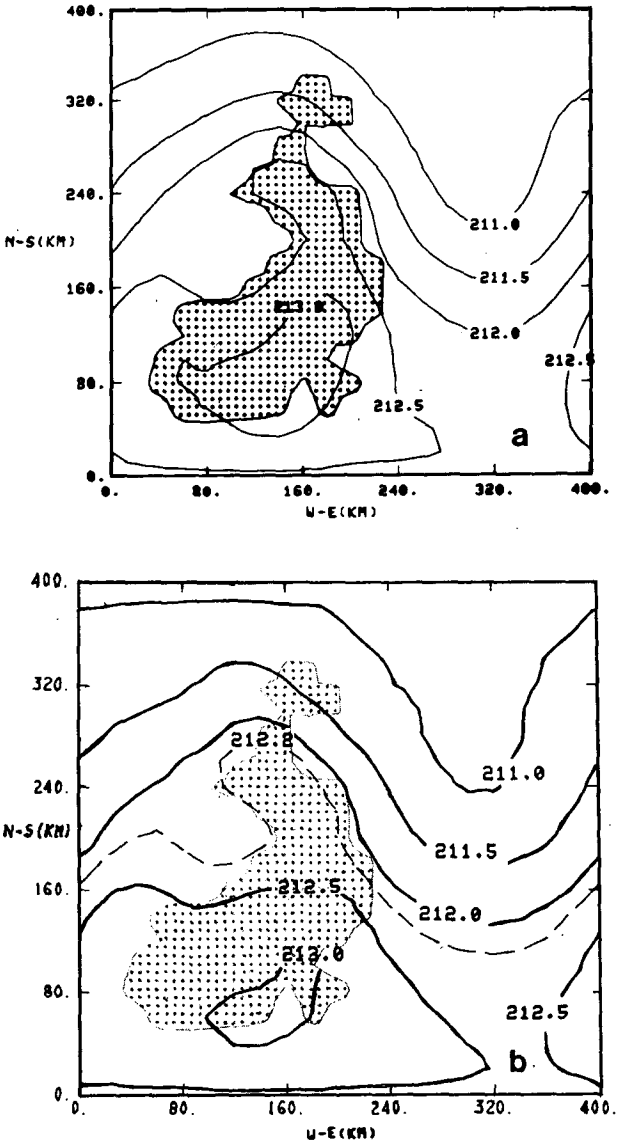

FIG. 5. As in Fig. 3 except 75 min after convection began. In (a) cooling by overshooting cloud tops is included; in (b) it is omitted.

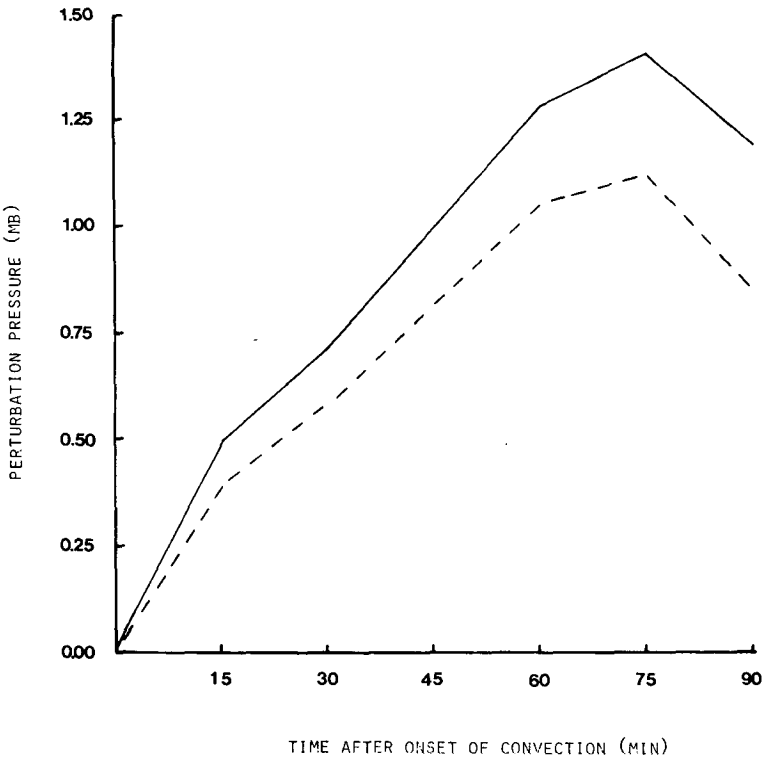

FIG. 6. Evolution of the maximum pressure perturbation. Solid line indicates "with cooling"; dashed line indicates "without." See text for definition of perturbation pressure.

tions of anomalously low temperatures and an elevated tropopause above hurricanes (see also Gentry, 1967).

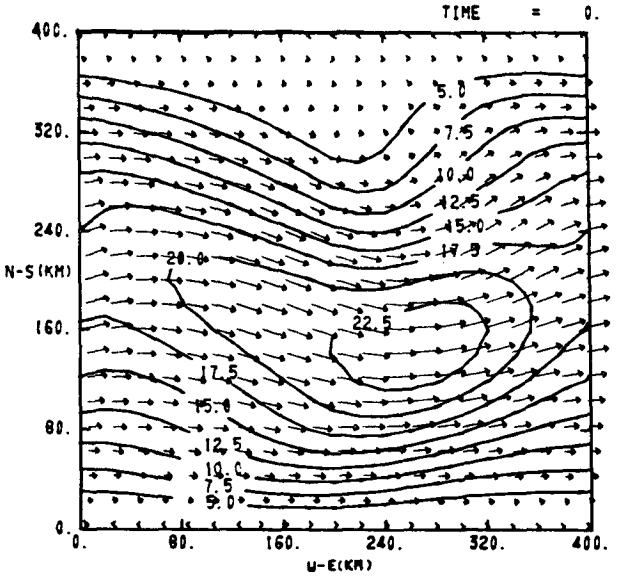

FIG. 7. Isotachs (m s^{-1}, solid lines) and wind direction (arrows) at 11.8 km level just prior to the onset of convection.

b. *Warming (on the mesoscale) of the middle and upper troposphere by deep convection*

This is the traditional explanation supported by the aforementioned linear analyses and results of tropical cyclone modeling. Moreover, the thermally-driven mesoscale, upward vertical circulation that develops in response to this warming will generally extend above it, thus contributing to local cooling near or above the tropopause. Arakawa (1951) attributed the existence of low temperatures aloft over a typhoon to this mechanism.

c. *Vertical transport of momentum by convection and mesoscale circulations*

Infusion of low-momentum air from the low troposphere into the upper troposphere and lower stratosphere by cumulonimbus or mesoscale updrafts, coupled with compensating subsidence of low-momentum air from the lower stratosphere, may cause partial blocking of the ambient flow near tropopause level. Perhaps through a Bernoulli-type effect, pressure and temperature perturbations result. This phenomena appears to have occurred in the three-dimensional simulations of thunderstorms by Klemp and Wilhelmson (1978).

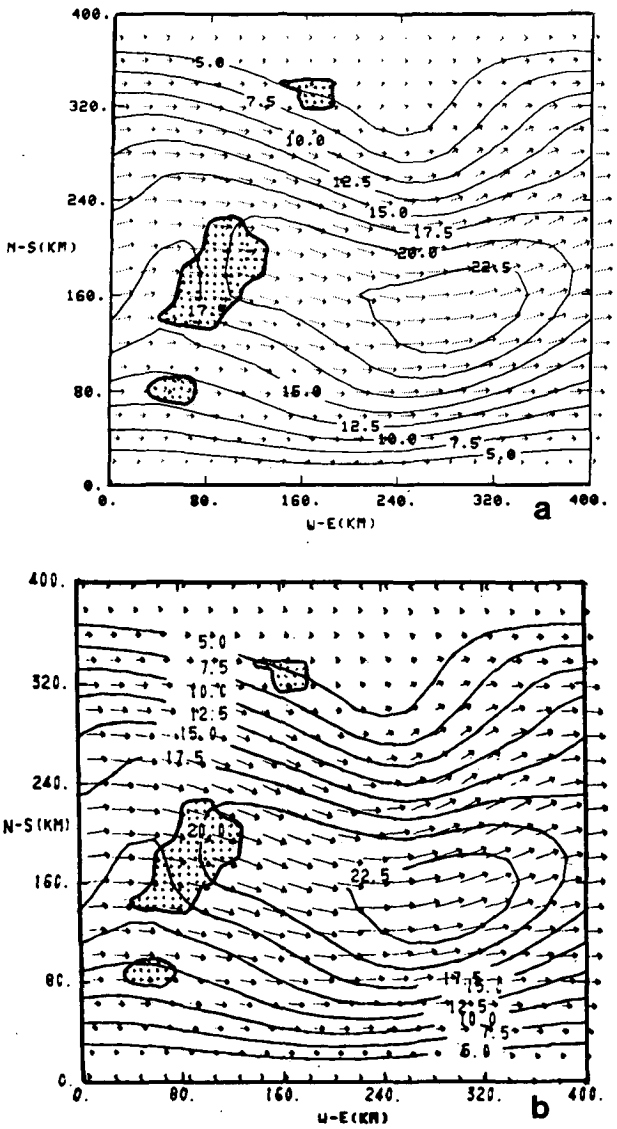

FIG. 8. Isotachs (m s^{-1}, solid lines), wind direction (arrows) and location of active convection (stippled) at 11.8 km level 30 min after convection began. In (a) cooling by overshooting cloud tops is included; in (b) it is omitted.

d. Radiative effects related to the presence of the extensive cirrostratus-altostratus canopy produced by intense convective systems

Webster and Stephens (1980) have shown that radiative effects tend to warm the base of this canopy and cool its top, with heating or cooling rates of 10°C day^{-1} or more. This vertical distribution will thus contribute to upper tropospheric mesohigh generation or amplification.

In an attempt to determine the relative contribution of the first of these mechanisms (direct incorporation of cold air into the lower stratosphere by overshooting cloud tops) to the production of the high-level mesohigh, two numerical simulations were performed; one including the introduction of cold air into the stratosphere and one in which the cooling was omitted. The results of these two simulations are shown in the following section. Section 4 briefly discusses some of the implications of the results.

3. Results of numerical simulations with and without cooling by overshooting convective cloud tops

A 20-level, primitive-equation model with 20 km horizontal resolution and a 400 km × 400 km domain (see Fritsch and Chappell, 1980b) was used to perform two numerical simulations of mesoscale convective systems to assess the contribution of over-

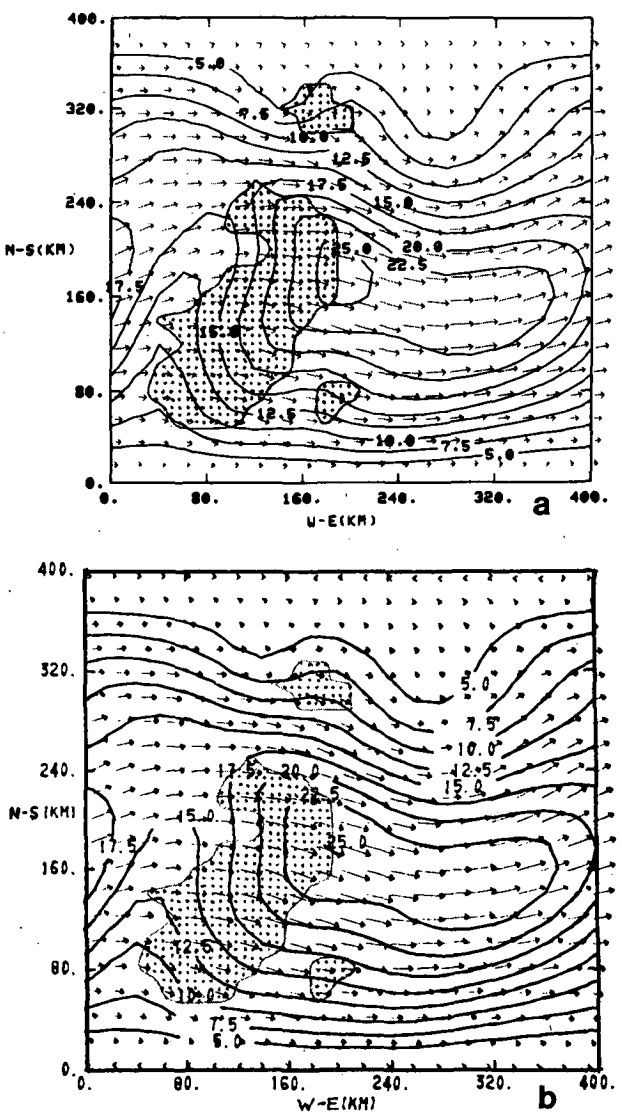

FIG. 9. As in Fig. 8 except 60 min after convection began.

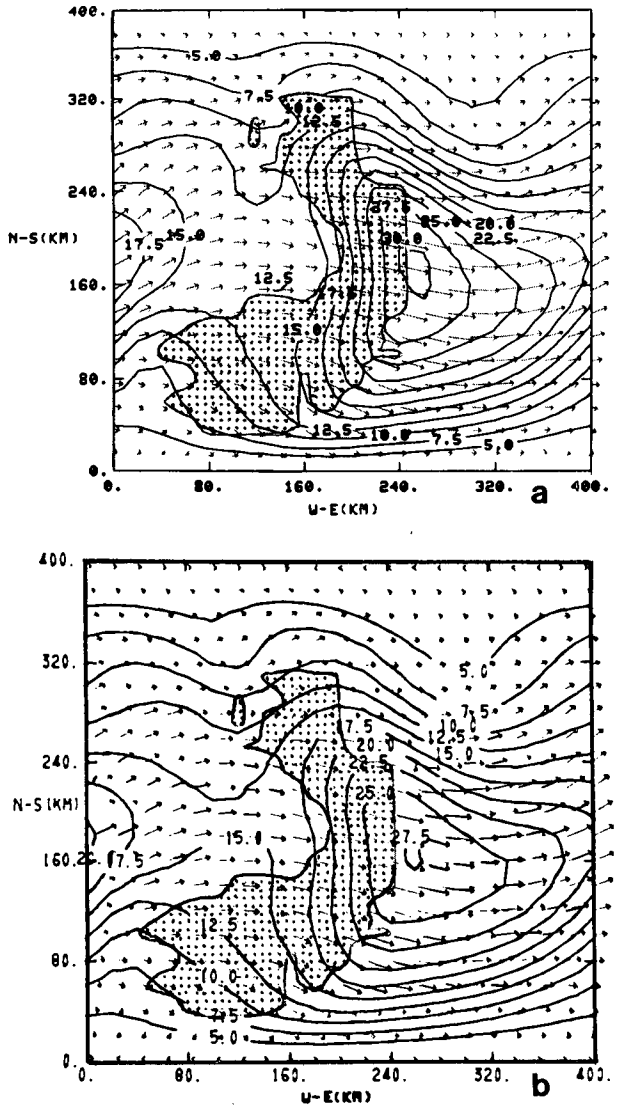

FIG. 10. As in Fig. 8 except 90 min after convection began.

shooting cloud-top cooling to the production of convectively-driven mesohighs aloft. The initial conditions and numerical simulations were identical in all respects except that in one simulation the cooling by overshooting cloud tops was omitted. Specifically, Fig. 2 shows a typical (for the model) vertical distribution of convective heating at a model grid point. The lightly shaded area centered around 14 km indicates the layer being cooled by the overshooting convective tops. Although in reality this layer is probably much thinner than indicated in Fig. 2, the model is unable to resolve the actual thickness and horizontal extent of the layer, so the cooling is artificially spread over the two highest model layers penetrated by the convective cloud tops. [The details of the convective parameterization and cloud model are presented in Fritsch and Chappell (1980a).] Furthermore, in addition to the discussion presented in Section 2a, it is assumed that successive cloud parcels overshoot in a more or less continuous (plume-like) manner. Thus, even though an overshooting parcel may become negatively buoyant, it cannot immediately and rapidly subside (e.g., as in the Brunt-Väisälä mode) because subsequent overshooting parcels rise into it and force it to spread out and subside more slowly. Cloud-top detrainment of cold air is therefore more of a mesoscale than cloud-scale process, and as such the redistribution of cold overshooting air is handled best by the governing primitive equations rather than by parameterizing it as a cloud-scale ef-

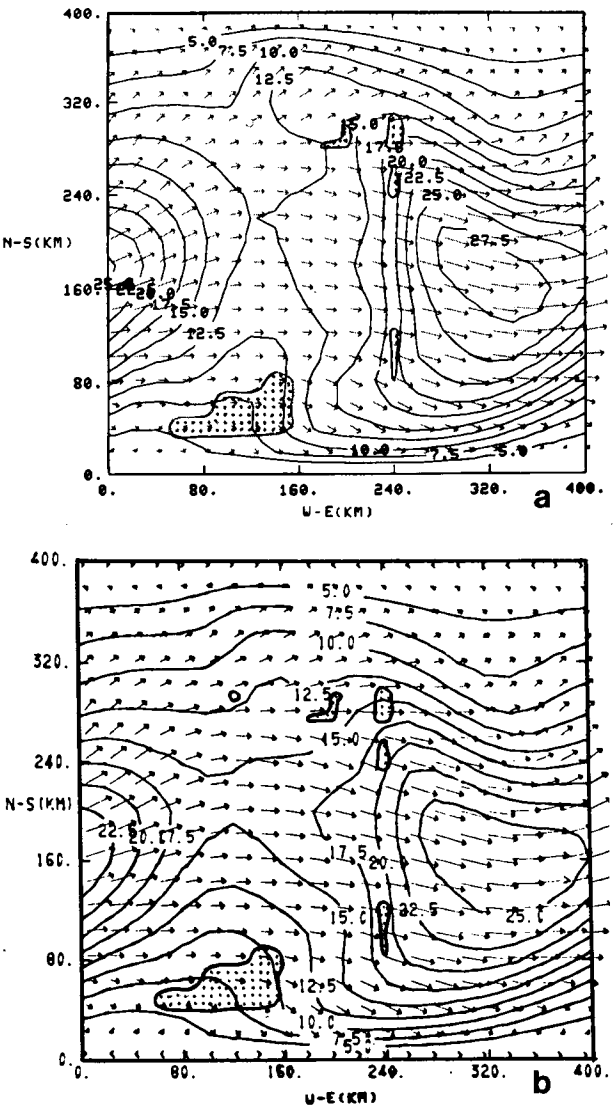

FIG. 11. As in Fig. 8 except 120 min after convection began.

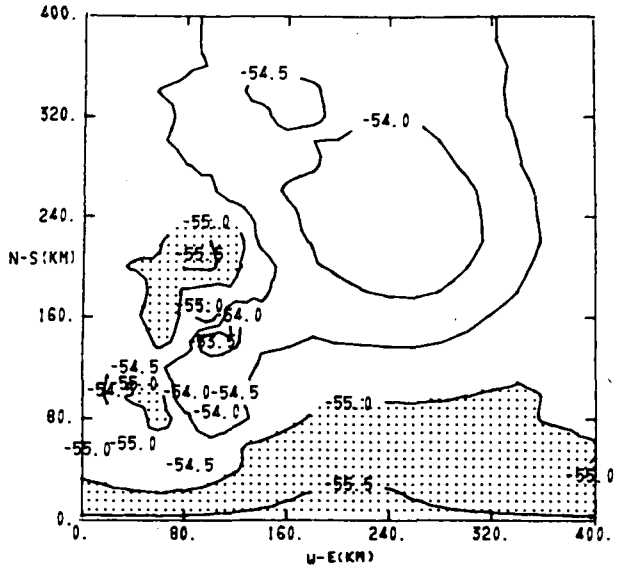

FIG. 12. Temperature field at 13.6 km level 45 min after convection began. Stippling indicates area with temperatures colder than −55°C. Cooling by overshooting cloud tops is omitted.

fect. In one of the simulations, this high-level layer of cooling by overshooting cloud tops is omitted at all grid points. However, the mass continuity calculations assuming penetration of the stratosphere are retained. Thus moisture and momentum transports by convective clouds and compensating subsidence are still included.

Fig. 3 shows the pressure field at the 11.8 km (~200 mb) level for both simulations (i.e., with and without high-level cooling) at about the time the convection begins. Figs. 4 and 5 show the subsequent evolution of the pressure field for both simulations. Note that, in general, there is little qualitative difference between the patterns; only the magnitude of the convectively forced perturbation is different. In order to quantify this change in magnitude of the pressure perturbation, thereby providing a measure of the impact of cooling by overshooting cloud tops, the maximum pressure and wind perturbations for each case were determined by graphically subtracting an unperturbed state (no convection) from the perturbed (with convection). The unperturbed state is estimated by simply advecting the initial wave (see Fig. 3) eastward until the axis of the trough is coincident with the axis of the trough of the perturbed wave. (In a control run where convection was not permitted to occur, the wave propagated eastward with little change in its basic structure or amplitude.) Fig. 6 shows the evolution of the maximum pressure perturbation for both cases, i.e., with and without cooling. At 45 min following the onset of convection, the pressure perturbations differ by about 0.2 mb; at 75 min the difference is ~0.3 mb. Thus, including cooling by overshooting cloud tops increases the pressure perturbation by about 25–30%. Moreover, this increased pressure perturbation is directly manifested in the wind field. For example, Fig. 7 shows the isotachs and streamflow of the wind at 11.8 km just prior to the onset of convection. Figs. 8–11 show the evolution of the wind for both simulations, i.e., with (a) and without (b) cooling. The perturbation wind speed (as defined above) was ~40% stronger when cooling was included. Also, in the "with-cooling" case, convection caused the *maximum* wind speed to increase by ~8 m s^{-1} over the initial maximum wind speed. In the "without-cooling" case, the increase in maximum wind speed was only about 5 m s^{-1} (compare Figs. 7 and 10).

The above results demonstrate that (within the model framework) cooling by overshooting cloud tops enhances mesohigh strength in the vicinity of the tropopause. While this is an interesting result, *it is perhaps more interesting that the mesohigh and associated wind perturbations still occur even when the cloud-top cooling is completely omitted*! It is important to point out, however, that this result does not of itself show that the production of a high-level cold pool can be removed from the list of potential mechanisms responsible for generation of elevated mesohighs. Rather, further examination of the without-cooling case reveals that a high-level cold pool formed in this case as well. Specifically, for the without-cooling simulation, Fig. 12 shows the temperature field at 13.6 km (~150 mb) level. Compare this field to the pressure field and location of active convection at the same time (Fig. 4b). Notice the cold

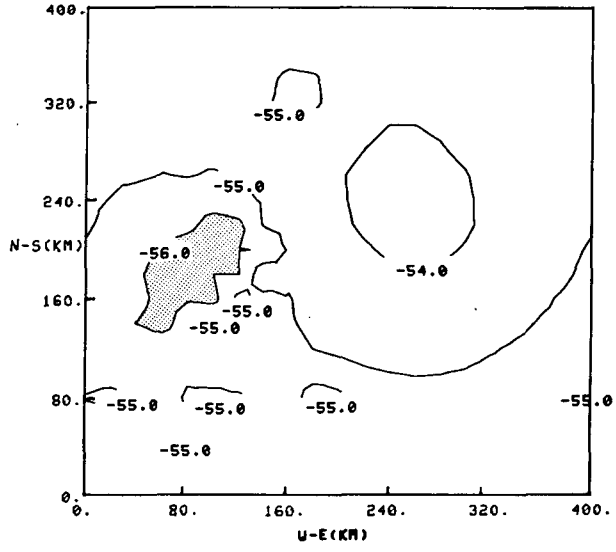

FIG. 13. As in Fig. 12 except cooling by overshooting cloud tops is included and shading indicates area with temperatures colder than −56°C.

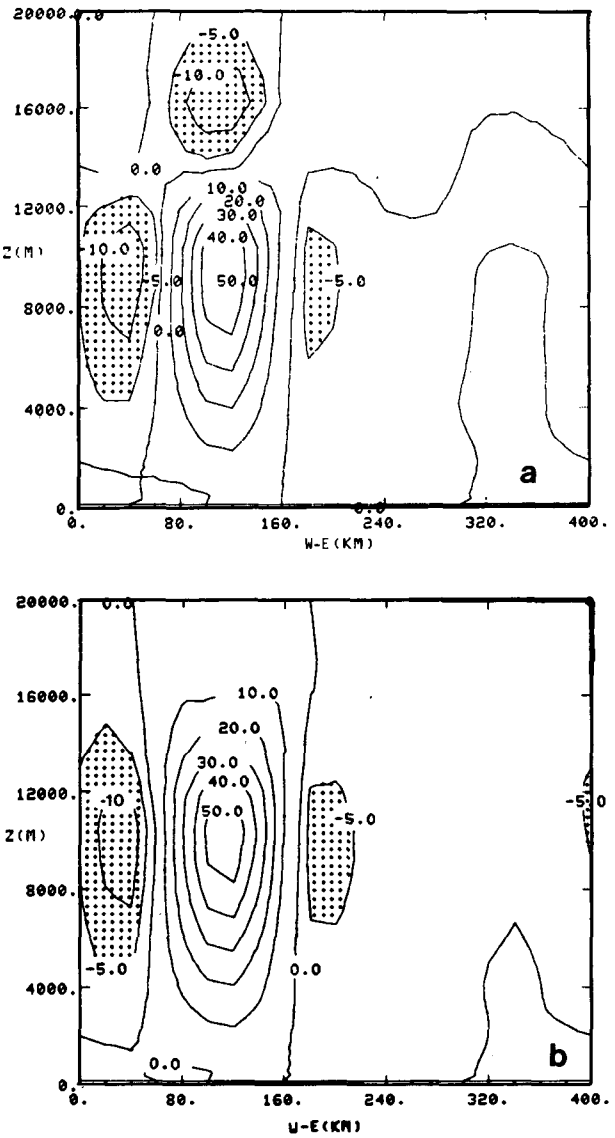

FIG. 14. Vertical cross section of vertical motion (cm s^{-1}) 45 min after convection began. Section passes east-west and was taken 100 km north of the origin (see Fig. 4a). In (a) cooling by overshooting cloud tops is included; in (b) it is omitted.

air pool above the largest region of active convection. A similar pool of cold air appeared above the region of deep convection in the with-cooling simulation (Fig. 13).

Within the governing constraints of the numerical model, the only mechanism which can account for the elevated cold pool in Fig. 12 is adiabatic expansion by vertical motion. In this regard, Figs. 14 and 15 show vertical and horizontal cross sections, respectively, of the *mesoscale* vertical motion that formed in response to the convective cloud heating (see Fig. 2). Notice that in each case the vertical circulation extends well through the 13.6 km level. Notice also, that the *without-cooling case developed substantially stronger mesoscale lifting at high levels* than the with-cooling case. Thus, even without the direct incorporation of cool air by overshooting cloud tops, the atmosphere, through scale interaction, is able to accomplish nearly the same result. Further, since the mesoscale ascent also extended to considerable heights in the with-cooling case, *it is likely that the production of the cold layer results from a combination of both processes, i.e., direct incorporation of overshooting cold outflow and cooling by adiabatic expansion in the mesoscale circulation.*

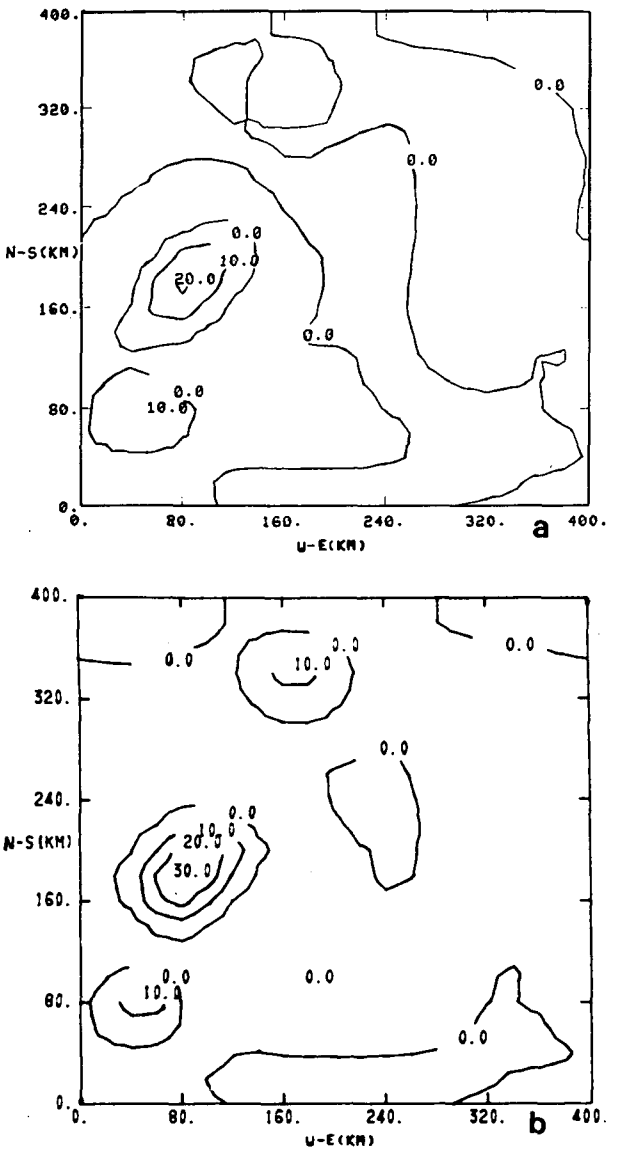

FIG. 15. Horizontal cross section of vertical motion (cm s^{-1}) at 13.6 km level, 30 min after convection began. Weak subsidence not shown; see Fig. 14a. In (a) cooling by overshooting cloud tops is included; in (b) it is omitted.

Finally, it is interesting that in this experiment, not only did the mesoscale vertical circulation extend to greater heights when overshooting cooling was omitted than when it was included, but the circulation was stronger as well. This effect is reflected in the total precipitation for the system; i.e., the without-cooling case produced ~10% more precipitation than the with-cooling case. How the omission of high-level cooling strengthens the vertical circulation is not readily apparent. Perhaps the cooling acts as a "drag" on the whole system since the mesoscale ascending circulation is forced to lift colder (heavier) air. Whatever the reason, it is clear that the interaction of deep convection with its environment is incredibly complex and additional experiments, focusing on the role of momentum (Section 2c) and radiation (Section 2d) in the generation of high-level mesohighs, must be conducted.

4. Concluding remarks

The results presented here suggest that while cooling of a layer of air in the vicinity of the tropopause may be accomplished directly by the infusion of cold, overshooting outflow (Section 2a), adiabatic expansion in a convectively forced region of mesoscale ascent (Section 2b) can accomplish the same result alone. Moreover, direct cooling by convection causes mesoscale subsidence which partly *negates* the cooling.

The increasing evidence for the existence and importance of a convectively driven mesoscale vertical circulation (Fankhauser, 1969, 1974; Yamasaki, 1975; Fritsch *et al.*, 1976; Sanders and Emanuel, 1977; Ogura and Chen, 1977; Kreitzberg and Perkey, 1977; Houze, 1977; Zipser, 1977; Leary and Houze, 1979, 1980; Brown, 1979; Johnson, 1980; Maddox, 1980b; Fritsch and Chappell, 1980b; Bosart and Sanders, 1981; Fritsch and Maddox, 1981a,b; Maddox *et al.*, 1981; Zipser *et al.*, 1981; Gamache and Houze, 1982) compounds the problem of how to parameterize the effects of deep convection in large-scale models. In particular, if transports by mesoscale circulations are systematically omitted in general circulation models, then the possibility clearly exists that long-term integrations will suffer from a cumulative error that may bound long-term predictability. Furthermore, the mesoscale circulation appears to be very sensitive to the vertical distribution of convective heating. Thus, great care must be taken in selecting a convective parameterization in order to ensure the proper magnitude and vertical distribution of convectively forced vertical transports.

Acknowledgments. The work was partially supported by the Bureau of Reclamation, Division of Atmospheric Water Resources. The manuscript was skillfully prepared by Betty Stoltz, Michele Shawver and Delores Corman.

REFERENCES

Arakawa, H., 1951: Analysis of the tropopause and the stratospheric field of temperature of a mature typhoon. *Pap. Meteor. Geophys.*, **2**, 1–5.

Black, P. G., and R. A. Anthes, 1971: On the asymmetric structure of the tropical cyclone outflow layer. *J. Atmos. Sci.*, **28**, 1348–1366.

Bosart, L. F., and F. Sanders, 1981: The Johnstown flood of July 1977: A long-lived convective system. *J. Atmos. Sci.*, **38**, 1616–1642.

Brown, J. M., 1979: Mesoscale unsaturated downdraft driven by rainfall evaporation: A numerical study. *J. Atmos. Sci.*, **36**, 313–338.

Deardorff, J. W., 1974: Three-dimensional numerical study of the height and mean structure of a heated planetary boundary layer. *Bound.-Layer Meteor.*, **7**, 81–106.

Fankhauser, J. C., 1969: Convective processes resolved by a mesoscale rawinsonde network. *J. Appl. Meteor.*, **8**, 778–798.

——, 1974: The derivation of consistent fields of wind and geopotential height from mesoscale rawinsonde data. *J. Appl. Meteor.*, **13**, 637–646.

Fett, R. W., 1966: Upper-level structure of the formative tropical cyclone. *Mon. Wea. Rev.*, **94**, 9–18.

Fritsch, J. M., and C. F. Chappell, 1980a: Numerical prediction of convectively driven mesoscale pressure systems. Part I: Convective parameterization. *J. Atmos. Sci.*, **37**, 1722–1733.

——, and ——, 1980b: Numerical prediction of convectively driven mesoscale pressure systems. Part II: Mesoscale model. *J. Atmos. Sci.*, **37**, 1734–1762.

——, and R. A. Maddox, 1981a: Convectively driven mesoscale weather systems aloft. Part I: Observations. *J. Appl. Meteor.*, **20**, 9–19.

——, and ——, 1981b: Convectively driven mesoscale weather systems aloft. Part II: Numerical simulations. *J. Appl. Meteor.*, **20**, 20–26.

——, C. F. Chappell and L. R. Hoxit, 1976: The use of large-scale budgets for convective parameterization. *Mon. Wea. Rev.*, **104**, 1408–1418.

Gamache, J. F., and R. A. Houze, Jr., 1982: Mesoscale air motions associated with a tropical squall line. *Mon. Wea. Rev.*, **110**, 118–135.

Gentry, R. C., 1967: Structure of the upper troposphere and lower stratosphere in the vicinity of hurricane Isabell, 1964. *Pap. Meteor. Geophys.*, **18**, 293–310.

Houze, R. A., 1977: Structure and dynamics of a tropical squall-line system. *Mon. Wea. Rev.*, **105**, 1540–1567.

——, and A. K. Betts, 1981: Convection in GATE. *Rev. Geophys. Space Phys.*, **19**, 541–576.

Johnson, R. H., 1980: Diagnosis of convective and mesoscale motions during Phase III of GATE. *J. Atmos. Sci.*, **37**, 733–753.

Jones, R. W., 1980: A three-dimensional tropical cyclone model with release of latent heat by the resolvable scales. *J. Atmos. Sci.*, **37**, 930–938.

Klemp, J. B., and R. B. Wilhelmson, 1978: Simulation of right- and left-moving storms produced through storm splitting. *J. Atmos. Sci.*, **35**, 1097–1110.

Koss, W. J., 1976: Linear stability analysis of CISK-induced disturbances: Fourier component eigenvalue analysis. *J. Atmos. Sci*, **33**, 1195–1222.

Kotswaram, P., 1967: On the structure of hurricanes in the upper troposphere and lower stratosphere. *Mon. Wea. Rev.*, **95**, 541–564.

Kreitzberg, C. W., and D. J. Perkey, 1976: Release of potential instability: Part I. A sequential plume model within a hydrostatic primitive equation model. *J. Atmos. Sci.*, **33**, 456–475.

——, and ——, 1977: Release of potential instability: Part II. The mechanism of convective/mesoscale interaction. *J. Atmos. Sci.*, **34,** 1569–1595.

Leary, C. A., 1979: Behavior of the wind field in the vicinity of a cloud cluster in the intertropical convergence zone. *J. Atmos. Sci.*, **36,** 631–639.

——, and R. A. Houze, Jr., 1979: The structure and evolution of convection in a tropical cloud cluster. *J. Atmos. Sci.*, **36,** 437–457.

——, and ——, 1980: The contribution of mesoscale motions to the mass and heat fluxes of an intense tropical convection system. *J. Atmos. Sci.*, **37,** 784–796.

Maddox, R. A., 1980a: Mesoscale convective complexes. *Bull. Amer. Meteor. Soc.*, **61,** 1374–1387.

——, 1980b: An objective technique for separating macroscale and mesoscale features in meteorological data. *Mon. Wea. Rev.*, **108,** 1108–1121.

——, D. J. Perkey and J. M. Fritsch, 1981: Evaluation of upper-tropospheric features during the development of a meso-scale convective complex. *J. Atmos. Sci.*, **38,** 1664–1674.

Ninomiya, K., 1971a: Dynamical analysis of outflow from tornado-producing thunderstorms as revealed by ATS III pictures. *J. Appl. Meteor.*, **10,** 275–294.

——, 1971b: Mesoscale modification of synoptic situations from thunderstorm development as revealed by ATS III and aerological data. *J. Appl. Meteor.*, **10,** 1103–1121.

Ogura, Y., and Y. Chen, 1977: A life history of an intense mesoscale convective storm in Oklahoma. *J. Atmos. Sci.*, **34,** 1458–1476.

Ooyama, K., 1969: Numerical simulation of the life cycle of tropical cyclones. *J. Atmos. Sci.*, **26,** 3–40.

Riehl, H., 1959: On production of kinetic energy from condensation heating. *The Atmosphere and the Sea in Motion*, Rockefeller Institute Press, 381–399.

Rosenthal, S. L., 1969: A circularly symmetric primitive equation model of tropical cyclone development containing an explicit water vapor cycle. *Mon. Wea. Rev.*, **98,** 643–663.

Sanders, F., and K. A. Emanuel, 1977: The momentum budget and temporal evolution of a mesoscale convective system. *J. Atmos. Sci.*, **34,** 322–330.

Syōno, S., and M. Yamasaki, 1966: Stability of symmetrical motion driven by latent-heat release by cumulus convection under the existence of surface friction. *J. Meteor. Soc. Japan*, **44,** 353–375.

Webster, P. J., and G. L. Stephens, 1980: Tropical upper tropospheric extended clouds: Inferences from winter MONEX. *J. Atmos. Sci.*, **37,** 1521–1541.

Yamasaki, M., 1975: A numerical experiment of the interaction between cumulus convection and larger-scale motion. *Pap. Meteor. Geophys.*, **26,** 63–91.

Yanai, M., 1964: Formation of tropical cyclones. *Rev. Geophys.*, **2,** 367–414.

Zipser, E. J., 1977: Mesoscale and convective scale downdrafts as distinct components of squall-line structure. *Mon. Wea. Rev.*, **105,** 1568–1589.

——, R. J. Meitin and M. A. Lemone, 1981: Mesoscale motion fields associated with a slowly moving GATE convective band. *J. Atmos. Sci.*, **38,** 1725–1750.